Polymer Degradation and Stability 230 (2024) 111017

Contents lists available at ScienceDirect

Polymer Degradation and Stability

journal homepage: www.journals.elsevier.com/polymer-degradation-and-stability

Development of flame retardant coatings containing hexaphenoxycyclotriphosphazene and expandable graphite for carbon fibre-reinforced polyamide 6 composites

Zsófia Kovács [a,b], Andrea Toldy [a,b,*]

[a] Department of Polymer Engineering, Faculty of Mechanical Engineering, Budapest University of Technology and Economics, Műegyetem rkp. 3, Budapest H-1111, Hungary
[b] MTA-BME Lendület Sustainable Polymers Research Group, Műegyetem rkp. 3, Budapest H-1111, Hungary

ARTICLE INFO

Keywords:
Flame retardancy
Hexaphenoxycyclotriphosphazene
Expandable graphite
In-mould coating
Polyamide 6 composites
In-situ polymerisation

ABSTRACT

The increasing importance of thermoplastic composites, driven by their enhanced recyclability and production efficiency, has attracted interest in continuous fibre-reinforced thermoplastic. Polyamide 6 (PA6), synthesised via anionic ring-opening polymerisation, is particularly relevant, however, the flammability of PA6 poses significant challenges and a critical concern for their structural application, necessitating effective flame retardancy measures. This study investigates the development of flame retardant coatings for carbon fibre-reinforced PA6 composites, employing hexaphenoxycyclotriphosphazene (HPCTP) and expandable graphite (EG), and evaluates their efficacy in improving the flammability properties of the composites through their combined modes of action. We investigated the impact of FRs on glass transition temperature, crystallinity, thermal stability, monomer conversion and flammability properties. The best-performing formulations (PA6/3P%HPCTP/3%EG and PA6/3P%HPCTP/4%EG) were applied to the surface of carbon fibre-reinforced PA6 composites by in-mould coating. Due to the synergistic effect of HPCTP and EG, the coatings containing 3P% HPCTP and 3 % EG reduced the maximum heat release by 33 % and the total heat release by 37 %.

1. Introduction

Nowadays, thermoplastic composites are becoming increasingly significant, as the recyclability of traditional crosslinked composites is limited and challenging. On the other hand, thermoplastic polymer composites offer enhanced recyclability and production efficiency due to their low cycle times [1]. While injection moulding and extrusion have long been used for manufacturing short-fibre composite products, continuous fibre-reinforced thermoplastic composites have emerged more recently. A particularly effective method for their production is thermoplastic resin transfer moulding (T-RTM), where a low-viscosity monomer is injected into the mould, and polymerisation occurs between the reinforcing materials [2–4]. Polyamide 6, produced by anionic ring-opening polymerisation of caprolactam monomer in the presence of an initiator and activator [5], stands out as a significant polymer that can be processed with T-RTM. One of the main applications for products made with T-RTM is in the automotive industry, where one of the main goals is to produce fibre-reinforced composites with short cycle times. In the case of anionic ring-opening polymerisation, the short polymerisation time makes the resulting products suitable for mass production [6]. Furthermore, an additional advantage of composite products made with T-RTM is that the thermoplastic matrix allows them to be remelted after shredding and reprocessed using conventional technologies (compression moulding, extrusion-compression moulding, injection moulding) [7].

One of the drawbacks of using polymer composites is that they are highly flammable, which can be a critical factor in structural composite applications. This is particularly true for thermoplastic polymers that are thermally less stable and prone to dripping, so their proper flame retardancy is essential. However, several problems can arise during the flame retardancy of composites. In particular, in carbon fibre-reinforced composites, the high thermal conductivity of the carbon fibres results in a phenomenon known as the candlewick effect. The reinforcing material is able to transfer and return the heat of combustion to the matrix and

* Corresponding author at: Department of Polymer Engineering, Faculty of Mechanical Engineering, Budapest University of Technology and Economics, Műegyetem rkp. 3, Budapest H-1111, Hungary.
E-mail address: atoldy@edu.bme.hu (A. Toldy).

https://doi.org/10.1016/j.polymdegradstab.2024.111017
Received 19 June 2024; Received in revised form 19 September 2024; Accepted 22 September 2024
Available online 22 September 2024

Table 1
The conversion of HPCTP in PA6 samples from mass% to P%.

Sample	HPCTP [g/100 g]	P-content [%]
PA6/1P% HPCTP	7.46	1
PA6/2P% HPCTP	14.9	2
PA6/3P% HPCTP	22.38	3
PA6/4P% HPCTP	29.85	4

the fuels from matrix pyrolysis by capillary action to the flame, leading to continuous and intensive burning [8]. Furthermore, carbon layers may filter out the solid particulate flame retardants during the composite manufacturing processes like infusion, resulting in an uneven distribution of flame retardants, and consequently unpredictable fire performance. Additionally, in the case of flame retardants acting in the condensed phase, the formation of a protective layer may be prevented by the reinforcing material; instead, the flame retarded matrix layers between the reinforcements just result in a delamination, leading to the deterioration of the post-fire mechanical properties. These problems can be solved by applying a flame retardant coating on the surface of the composite [9,10]. In addition to traditional coating technologies (spraying, brushing), in-mould coating, created in a closed mould, is an option [11]. Our recent review article details the difficulties and solutions related to the flame retardancy of caprolactam-based PA6 [9].

Phosphazenes are organic-inorganic hybrid polymers consisting of a backbone of alternating phosphorus and nitrogen atoms [12,13]. Recently, phosphazene-based compounds have been discovered to have remarkable properties, including enhanced thermal-oxidative stability and flame retardancy. They have a predominant gas phase flame retardant action due to the formed phosphorus-containing radicals. At the same time, the released inflammable gases, including CO_2, NH_3 and N_2, dilute the oxygen supply, while the phosphates, metaphosphates and polyphosphates generated during the thermal decomposition form a protective layer on the polymer surface that prohibits mass and heat transfer.; thus, the combination of various mechanisms contributes to their flame retardant effect [14]. Hexaphenoxycyclotriphosphazene (HPCTP) is a member of the cyclic phosphazene compounds family [15]. HPCTP exhibits good thermal stability and flame retardancy due to its phosphorus and benzene ring structures. It is used in a variety of materials including polyethylene (PE) [16], rigid polyurethane foam (RPUF) [17], epoxy [18] and silicone rubber [19,20]. HPCTP is an effective flame retardant for PA6 [21,22]. Furthermore, as HPCTP is soluble in molten CL and does not inhibit the polymerisation of caprolactam, it can be used as a flame retardant during *in-situ* polymerisation [23,24].

Expandable graphite (EG) is a form of graphite that has undergone partial oxidation, resulting in intercalated compounds, such as sulfuric acid anions, between the stacked graphene layers [25,26]. Upon being subjected to high temperatures beyond a specific expansion onset temperature, expandable graphite exhibits a distinctive characteristic of exfoliating. This property is the primary feature of this material. The exfoliation process leads to a rapid expansion of the graphite in a worm-like manner, resulting in the formation of graphite with a low density [27]. EG has proven to be an excellent flame-retardant additive in various polymers, including PA6 [28–31].

EG has also been combined with phosphorus-containing HPCTP in several materials [32–35], as a synergistic effect can be achieved when used together. The phosphorus compounds act in the condensed and gas phases, whereas the expandable graphite acts in the condensed phase. When combined, the flame retardants form a char layer, the main effect of which is heat shielding, based on the increased reradiation by the surface with a much higher temperature than non-charring burning.. In addition, as the temperature increases, the phosphorus begins to oxidise, and various P-containing groups are formed, which can react further with the graphite in the char layer when exposed to oxygen and heat. This contact prevents the formation of cracks in the protective layer.

This research aims to develop PA6-based flame retardant coatings for carbon fibre-reinforced PA6 composites. In our previous research [36], red phosphorus and magnesium oxide were mixed with expandable graphite and used as flame retardants in the coating. The coatings reduced the maximum peak heat release by up to 27 % and the total heat release by 37 %. However, none of the flame retardants were soluble in the caprolactam, so soluble HPCTP was used in the present study. As a first step of the study, the effects of HPCTP on the thermal and flammability properties of PA6 and monomer conversion were investigated. When used alone, HPCTP was effective, but did not show outstanding results, so it was combined with EG acting in the condensed phase. The best-performing compositions in terms of combustibility were applied to the surface of PA6 composites by in-mould coating. Finally, we investigated the flammability of the coated composites.

2. Materials and methods

2.1. Materials

The monomer used was ε-caprolactam, specifically the *AP-NYLON Caprolactam* type (CL, L. Brüggemann GmbH & Co. KG, Heilbronn, Germany). As an activator, we used the *Bruggolen C20P* type hexamethylene-1,6-dicarbamoyl caprolactam (C20, L. Brüggemann GmbH & Co. KG, Heilbronn, Germany). As for the initiator, we employed sodium dicaprolactamato-bis-(2-methoxyethoxo)-aluminate, commercially known as *Dilactamate* (DL), which was produced by Katchem (Prague, Czech Republic). Before use, both CL and C20 were stored under vacuum at 40 °C. The flame retardants used were hexaphenoxycyclotriphosphazene branded *Rabitle FP-110* (HPCTP, Fushimi Pharmaceutical Co Ltd., Japan) and *ES100 C10* type expandable graphite (EG, Graphit Kropfmühl, Hauzenberg, Germany). The phosphorus content of HPCTP is 13.4 %. For the phosphorus-containing flame retardant, we gave the amount of the additive in the sample in terms of phosphorus percentage (P%) instead of mass per cent (mass%). The conversion of HPCTP in PA6 samples from mass% to P% is summarised in Table 1. The chemical structure of CL, C20, DL and HPCTP are shown in Fig. 1. We used *PX 35 UD 300* type unidirectional carbon fibre reinforcement (CF, Zoltek LtD., Nyergesújfalu, Hungary) for the composites. The aereal weight of the CF reinforcement is 333 g/m^2.

2.2. Preparation of flame retardant PA6 coating materials

The initial step involved investigating the impact of flame retardants on the thermal properties and flammability of PA6. At first, PA6 samples were prepared without reinforcing materials, and only the most effective formulations were utilised as coatings on PA6 composites. The reference PA6, based on ε-caprolactam, was prepared using 87 mass% CL, 3 mass % C20, and 10 mass% DL. A thermoplastic resin transfer moulding (T-RTM) was modelled with a simplified small-scale process using an aluminium mould preheated in a 150 °C oven. The monomer, activator, and, in the case of flame retarded samples, the flame retardant(s) were mixed and melted at 120 °C using an MR Hei-TEC type (Heidolph, Germany) heated magnetic stirrer. Following the addition of the initiator, test specimens were prepared according to standard flammability tests. Mass loss type cone calorimetry was conducted on samples with dimensions of 100×100×4 mm^3, while UL-94 tests and oxygen index measurements were performed on specimens measuring 120×10×4 mm^3. A flow chart of the sample preparation is shown in Fig. 2.

2.3. Preparation of carbon fibre-reinforced PA6 composites

A mould with dimensions of 100×100×2 mm^3 was used to produce the composites. The unidirectional CF reinforcement was arranged in the mould in $[0]_5$ layup. The mould, containing the reinforcing material, was preheated in a drying oven at a temperature of 150 °C. The CL-based PA6 matrix was formulated by combining 87 mass% CL, 3 mass% C20,

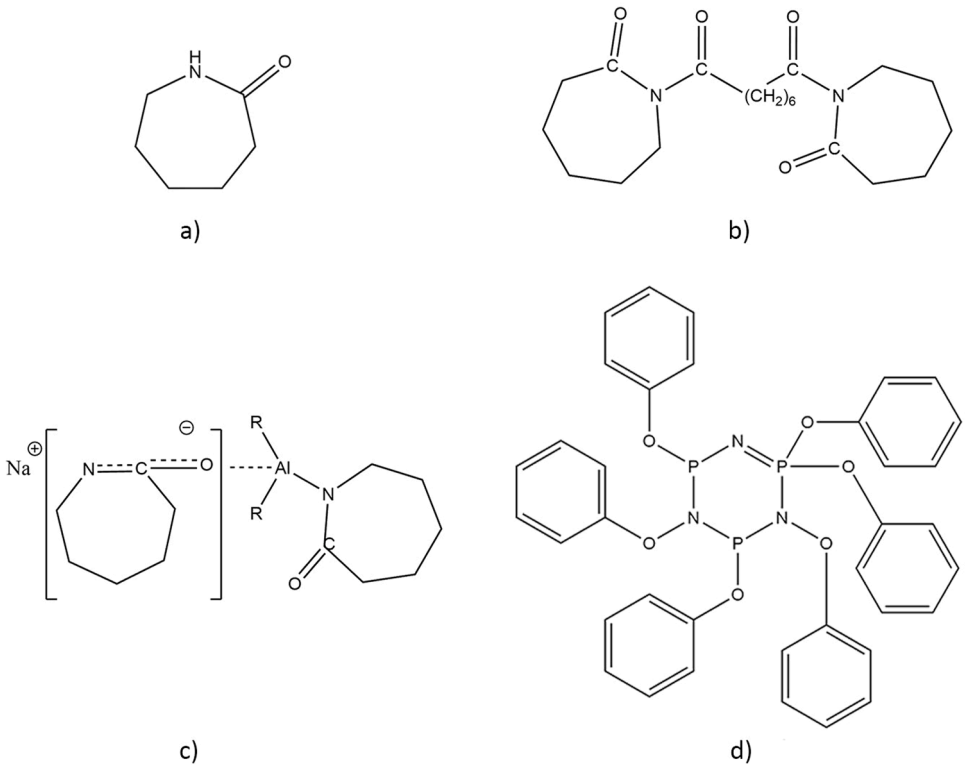

Fig. 1. Chemical structure of ε-caprolactam a), C20 activator b), Dilactamate initiator c), and hexaphenoxycyclotriphosphazene d).

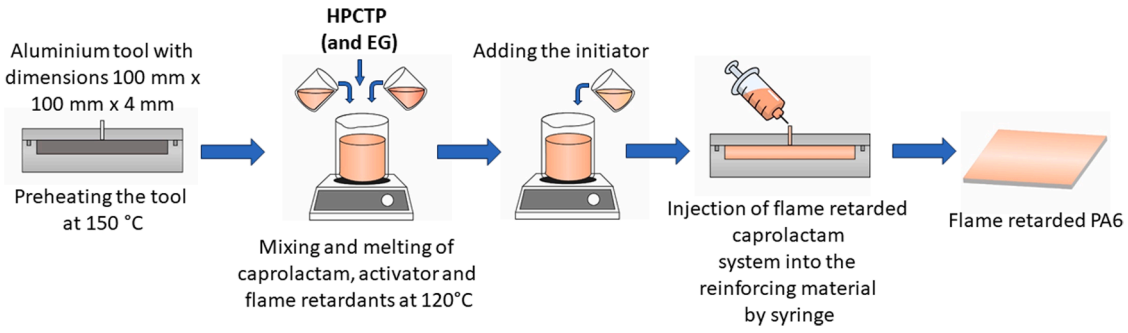

Fig. 2. Preparation of flame retarded PA6.

and 10 mass% DL. The mixture of ε-caprolactam and the activator was melted at a temperature of 120 °C and then mixed using an MR Hei-TEC type (manufactured by Heidolph, Germany) magnetic stirrer. Following the addition of the initiator, the molten mixture was injected into the closed mould using a Hamilton syringe (1025 TLL 25 ml SYR) to ensure sufficient pressure. After 15 min, the mould was removed from the drying oven. With this technology, we have achieved 50 mass% fibre content. The process for the production of the composite is shown in Fig. 3.

2.4. Preparation of flame retardant coatings on the surface of PA6 composites

An aluminium mould measuring 100×100×2.5 mm^3 was used to carry out IMC. The composite material was pre-positioned within the mould. Subsequently, the mould was sealed and preheated in a drying oven set at 150 °C. To generate a coating with a thickness of 0.5 mm, CL was melted at a temperature of 120 °C in the presence of an activator and flame retardant. This process was carried out using an MR Hei-TEC type (Heidolph, Germany) heated magnetic stirrer. Following the addition of the initiator, the melted ε-caprolactam system was introduced into the sealed mould using a Hamilton syringe. After 15 min, the mould was removed from the drying oven. The IMC process is presented in Fig. 4.

2.5. Characterisation

The glass transition temperatures and the crystalline fraction of the reference and flame retarded PA6 samples were measured using a TA Instruments Q2000 (New Castle, DE, USA) differential scanning calorimeter (DSC). Samples of 5–10 mg were analysed in a 50 ml/min N_2 flow. Heating-cooling-heating cycle measurements were performed at 25–250 °C. The heating and cooling rate was 10 °C/min.

Thermogravimetric analysis (TGA) was used to study thermal stability and monomer conversion. TA Instruments Q500 (New Castle, DE, USA) device was used for the test, with a 30 ml/min flow rate under the N_2 atmosphere at a heating rate of 20 °C/min between 30 and 600 °C. 5–10 mg of samples were used in the tests.

In UL-94 flammability testing (ISO 9772, ISO 9773), the flame spread rate was determined in the horizontal arrangement (H-type) and the

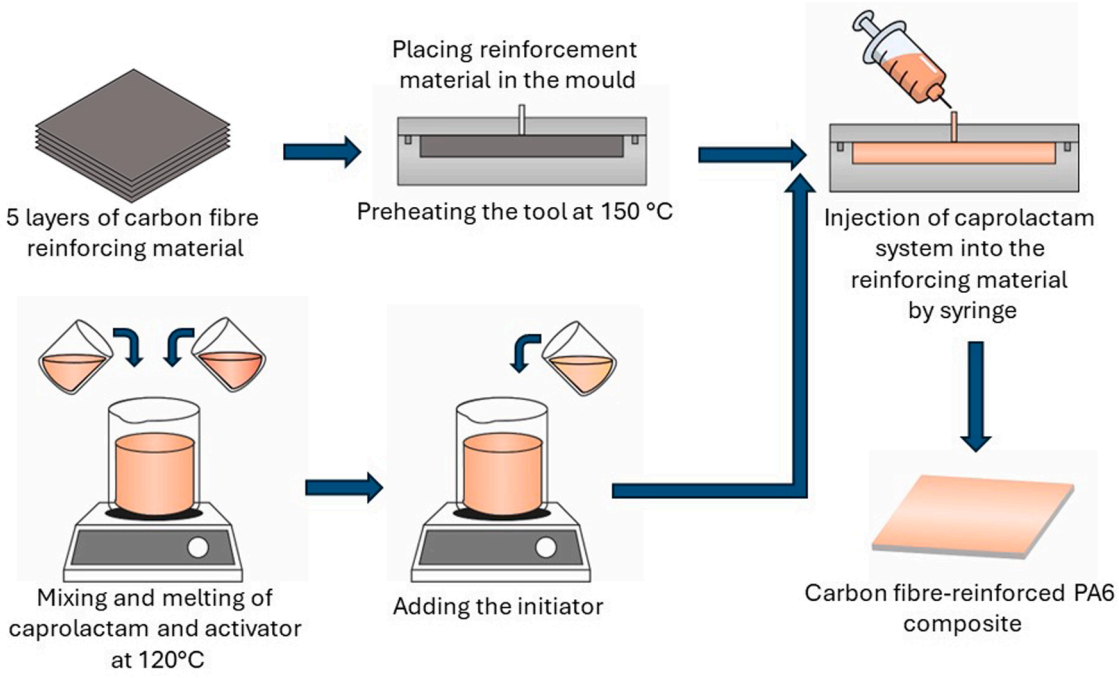

Fig. 3. Composite production process.

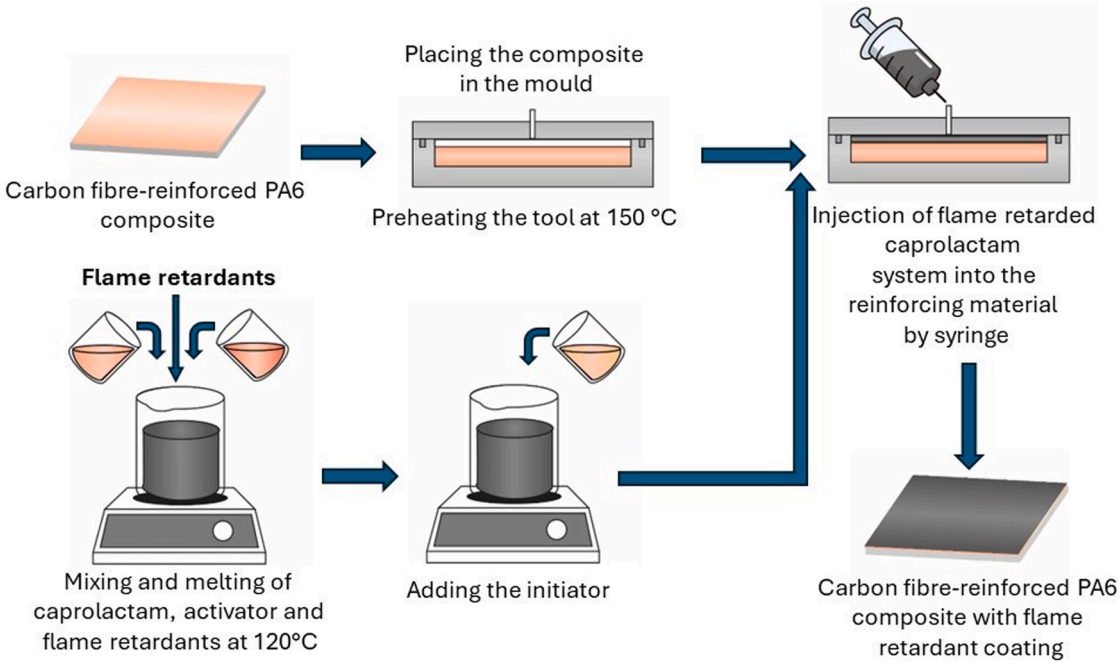

Fig. 4. Process of the in-mould coating (IMC).

flammability classification in the vertical arrangement (V-type). The samples used for the test were 120×10×3 mm^3.

We performed oxygen index tests (LOI) according to ISO 4589–1 and ISO 4589–2 standards. The oxygen index is the minimum oxygen content by volume of an oxygen-nitrogen gas mixture flowing at a specified velocity in the test sample that is still burning. The dimensions of the samples used for the test were 120×10×3 mm^3.

Mass loss type cone calorimetry (MLC, Fire Testing Technology, East Grinstead, UK) was used to determine the complex combustion characteristics of the samples. Samples with a surface area of 100×100 mm^2 were subjected to a heat flux of 50 kW/m^2. When testing the reference and flame retarded samples without reinforcement (the coating compositions), the sample size was 100×100×4 mm^3, while the reference PA6 composite size was 100×100×2 mm^3, and the coated composites were 100×100×2.5 mm^3. A spark ignition unit assisted in the ignition of the specimen surfaces. We determined the time to ignition (TTI), total heat release (THR), peak heat release rate (pHRR), and the time to pHRR, total burn time, and residual mass.

We investigated the residue of the reference and flame retarded samples after the MLC measurements using a JEOL JSM 6380LA type scanning electron microscope (SEM, Jeol Ltd., Tokyo, Japan). The SEM samples were coated with gold with a Jeol JPC1200 cathodic sputtering

Table 2
The results of DSC for reference and flame retarded PA6 samples (T_g: glass transition temperature; T_m: melting temperature; ΔH_m: melting enthalpy for the first heating; ΔH_c: enthalpy of crystallisation; X_c: crystalline fraction; Average standard deviation of the temperature measurements: ± 0.5 °C).

Sample	T_g [°C]	ΔH_m [J/g]	T_m [°C]	ΔH_c [J/g]	X_c [%]
PA6	49	78.6	216	45.9	42
PA6/1P%HPCTP	48	86.9	217	44.8	50
PA6/2P%HPCTP	49	78.4	216	39.2	49
PA6/3P%HPCTP	48	76.0	215	39.0	52
PA6/4P%HPCTP	47	62.2	215	34.4	47

gold plating device.

3. Results and discussion

As a first step of the research, the effects of different flame retardant compositions on the glass transition temperature, crystallinity, thermal stability, monomer conversion and flammability of PA6 were investigated. The best-performing compositions were applied as coatings on the surface of carbon fibre-reinforced PA6 composites.

3.1. PA6 coatings containing HPCTP

Based on the literature [23], the access to the P atom in heterocyclic HPCTP is sterically hindered; therefore, it does not significantly interfere with the polymerisation reaction of CL. In addition, it is soluble in molten CL and thus can be appropriately used as a flame retardant during its *in-situ* polymerisation. Based on these results, PA6 samples containing HPCTP at different concentrations were investigated as the first step of this study.

3.1.1. Glass transition temperature and crystallinity

The effect of HPCTP on the glass transition temperature, the melting temperature and the crystallisation was investigated by DSC. The results obtained are summarised in Table 2, and DSC curves are shown in Fig. 5.

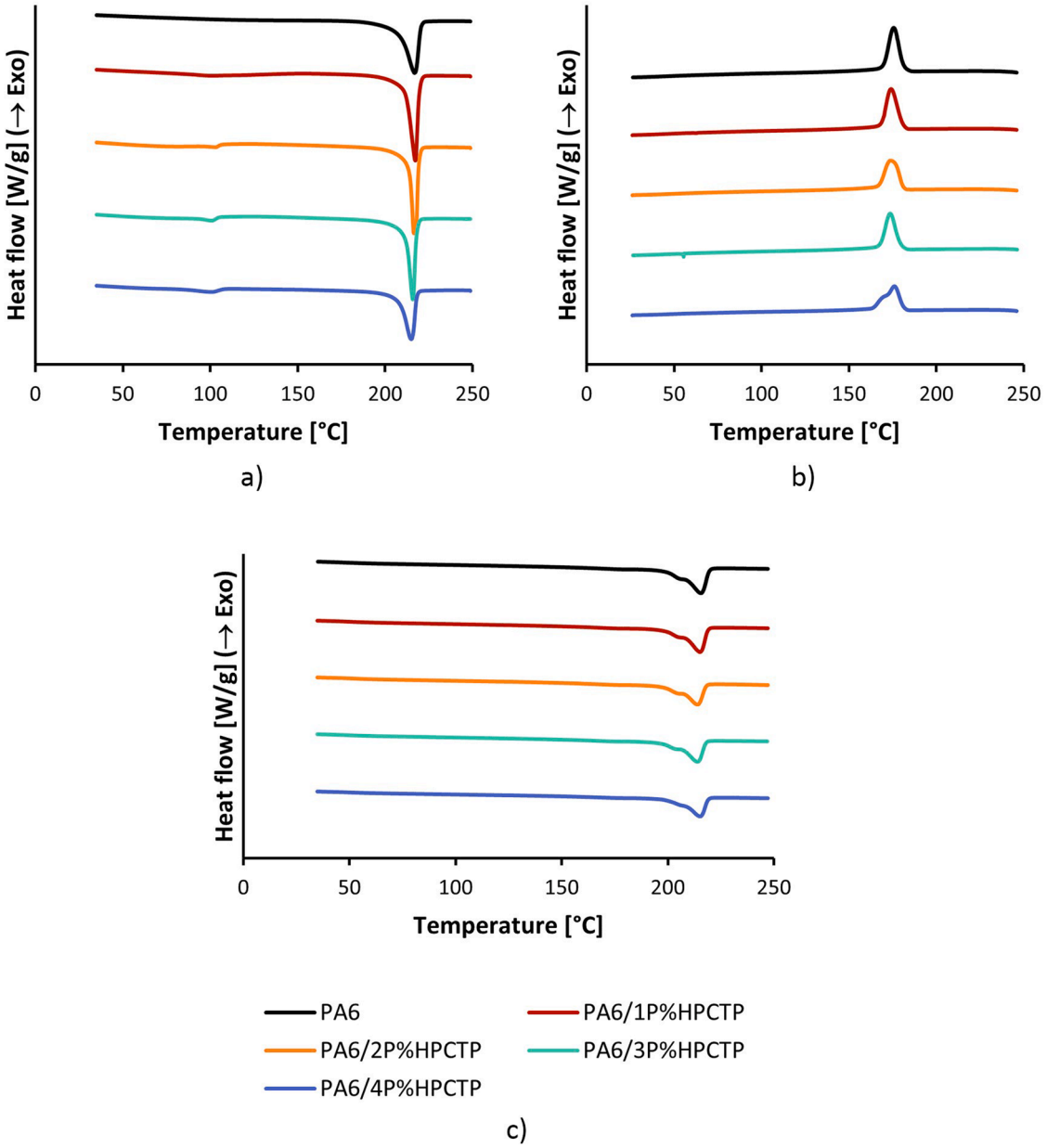

Fig. 5. DSC curves of HPCTP containing PA6, where (a) is the first heating, (b) is the cooling and (c) is the second heating.

Table 3
The results of TGA for PA6, caprolactam and flame retardants ($T_{-5\%}$: the temperature at 5% mass loss; $T_{-50\%}$: the temperature at 50 % mass loss; dTG_{max}: maximum decomposition rate; T_{dTGmax}: the temperature at the maximum decomposition rate; Average standard deviation values: temperature measurements: ± 0.5 °C, mass measurements: ± 1 %).

Sample	$T_{-5\%}$ [°C]	$T_{-50\%}$ [°C]	dTG_{max} [%/ °C]	T_{dTGmax} [°C]	Char yield at 600 °C [%]
PA6	241	341	2.2	338	2.0
CL	117	164	2.8	179	0.1
EG	228	-	0.4	228	75.7
HPCTP	311	371	1.7	381	0.5

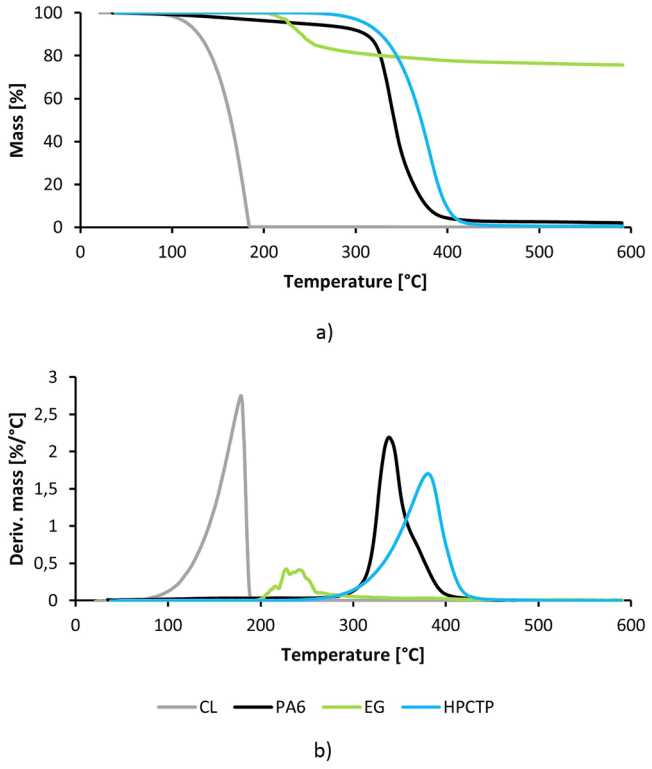

Fig. 6. TGA a) and DTG b) curves of ε-caprolactam (CL), polyamide 6 (PA6), expandable graphite (EG) and hexaphenoxycyclotriphosphazene (HPCTP).

Table 4
The results of TGA for flame retardant and reference PA6 samples ($T_{-5\%}$: the temperature at 5 % mass loss; $T_{-50\%}$: the temperature at 50 % mass loss; dTG_{max}: maximum decomposition rate; T_{dTGmax}: temperature corresponding to the maximum decomposition rate; Average standard deviation values: temperature measurements: ± 0.5 °C, mass measurements: ± 1 %).

Sample	$T_{-5\%}$ [°C]	$T_{-50\%}$ [°C]	dTG_{max} [%/ °C]	T_{dTGmax} [°C]	Char yield at 600 °C [%]	Monomer conversion [%]
PA6	241	341	2.2	338	2.0	97.5
PA6/1P% HPCTP	210	362	1.3	341	3.5	97.2
PA6/2P% HPCTP	214	351	1.7	339	1.6	97.5
PA6/3P% HPCTP	232	355	1.4	344	1.7	98.0
PA6/4P% HPCTP	258	347	1.3	341	1.3	98.8

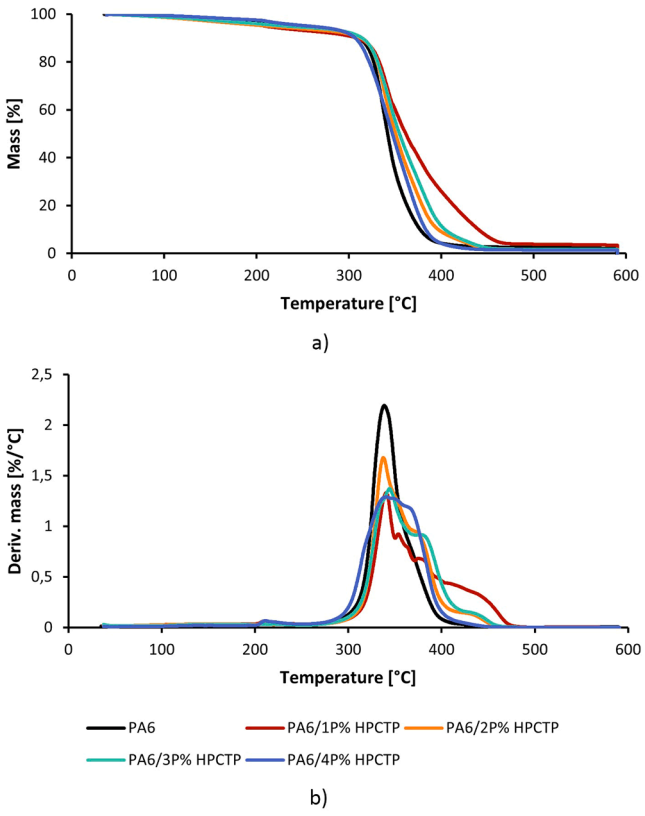

Fig. 7. TGA (a) and DTG (b) curves of polyamide 6 (PA6) with hexaphenoxycyclotriphosphazene (HPCTP).

Table 5
The results of UL-94 and LOI for reference and flame retardant coating materials (Average standard deviation of the LOI: ±1 vol%).

Sample	UL-94 ranking (burning rate)	LOI [%]
PA6	HB (24 mm/min)	21
PA6/1P%HPCTP	HB (18.9 mm/min)	22
PA6/2P%HPCTP	HB (10.3 mm/min)	22
PA6/3P%HPCTP	HB (6.9 mm/min)	24
PA6/4P%HPCTP	HB (6.1 mm/min)	25

For the DSC measurements, the glass transition temperature (T_g), the melting temperature (T_m), the melting enthalpy (ΔH_m), the enthalpy of crystallisation (ΔH_c) and the crystalline fraction (X_c) were determined.

We calculated the crystalline fraction (X_c) with Eq. (1), where ΔH_m is the enthalpy of crystallisation of the first heating curve, $\Delta H_{100\%}$ is the enthalpy of the melting if the polymer is 100 % crystalline, which for PA6 is $\Delta H_{100\%}$=188 J/g [37], and α is the flame retardant content.

$$X_c = \frac{\Delta H_m}{\Delta H_{100\%}(1-\alpha)} \cdot 100 \quad (1)$$

The glass transition temperature of the reference PA6 was 49 °C, while the melting temperature was 216 °C. DSC studies showed that neither the T_g nor the T_m was significantly affected by HPCTP. 1 P% HPCTP caused a slight increase in the melting enthalpy compared to the reference, but a decreasing trend in ΔH_m values was observed with increasing the amount of HPCTP. The melting enthalpy of the sample containing 4 P% HPCTP is 62.2 J/g, which is 21 % lower than that of the reference (78.6 J/g). A decrease in crystallisation enthalpy is also observed with increasing the amount of HPCTP due to the decreasing amount of PA6. The ΔH_c decreased from 45.9 J/g in the reference to 34.4 J/g with 4P% HPCTP. The crystalline fraction was lowest for the reference (42 %), with HPCTP increasing its value in all cases. According

Table 6
The results of MLC for reference and flame retardant coating materials (TTI: time to ignition, pHRR: peak heat release rate, THR: total heat release, FRI: flame retardancy index, MARHE: maximum average rate of heat emission, EHC: effective heat of combustion; Average standard deviation of the measured mass loss calorimeter values: TTI: ±3; pHRR: ±30; time to pHRR: ±5; residue: ±2).

Sample	TTI [s]	pHRR [kW/m^2]	time to pHRR [s]	THR [MJ/m^2]	Residue [%]	FRI [-]	MARHE [kW/m^{2}s]	EHC [MJ/kg]
PA6	19	1019	218	213	1.5	-	638	17
PA6/1P%HPCTP	20	975	210	197	0	1.2	602	16
PA6/2P%HPCTP	21	957	205	188	0	1.3	597	15
PA6/3P%HPCTP	23	987	202	182	0	1.4	557	14
PA6/4P%HPCTP	27	750	219	160	1.4	2.6	469	13

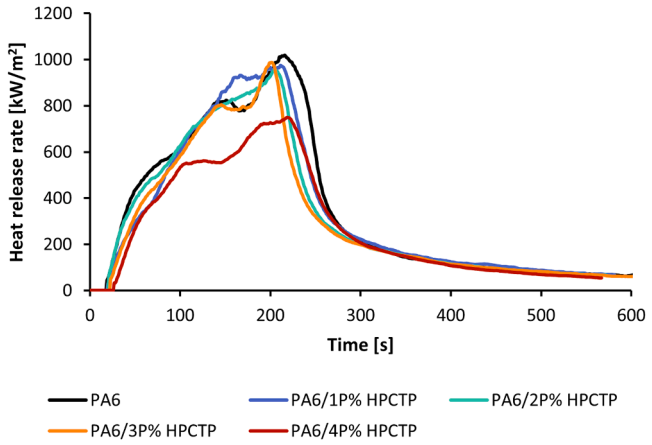

Fig. 8. The heat release rate of reference and flame retarded polyamide 6 (PA6) with different hexaphenoxycyclotriphosphazene (HPCTP) content.

Table 7
The results of DSC for reference and flame retarded PA6 samples (T_g: glass transition temperature; ΔH_m: melting enthalpy for the first heating; T_m: melting temperature; ΔH_c: enthalpy of crystallisation; X_c: crystalline fraction; Average standard deviation of the temperature measurements: ± 0.5 °C).

Sample	T_g [°C]	ΔH_m [J/g]	T_m [°C]	ΔH_c [J/g]	X_c [%]
PA6	49	78.6	216	45.9	42
PA6/3P%HPCTP	48	76.0	215	39.0	52
PA6/3P%HPCTP/1% EG	49	72.5	215	38.8	43
PA6/3P%HPCTP/2% EG	49	65.5	215	36.4	53
PA6/3P%HPCTP/3% EG	47	62.0	215	36.5	49
PA6/3P%HPCTP/4% EG	48	60.2	216	33.2	45
PA6/3P%HPCTP/5% EG	49	61.7	214	38.0	51

to the literature [22], even small amounts of HPCTP can be effective nucleation sites for PA6 molecules during crystallisation. HPCTP acts as a heterogeneous nucleating agent during this process, leading to the crystallisation of chain segments in the non-crystallisation region of PA6 and an acceleration in the crystallisation rate.

3.1.2. Thermal stability and monomer conversion

We investigated the thermal stability and the monomer conversion of PA6 samples containing HPCTP by TGA. The results obtained are shown in Table 3, including the temperature corresponding to 5 % and 50 % mass loss ($T_{-5\%}$ and $T_{-50\%}$), the maximum decomposition rate (dTG_{max}) and the corresponding temperature (T_{dTGmax}), and the char yield at 600 °C.

The monomer conversion reveals the potential presence of residual CL monomer in PA6 during anionic ring-opening polymerisation. Exploring the residual monomer content is crucial, given that the low molecular weight CL possesses plasticising properties that could potentially impact the mechanical characteristics of the end product. Therefore, we investigated first the possible overlap between the decomposition temperature of the flame retardants used in this research (HPCTP and EG) and the decomposition temperature of CL. The decomposition process of the flame retardants in the absence of PA6 was studied. Fig. 6 and Table 3 present the TGA results for CL monomer, PA6, HPCTP and EG.

The thermal decomposition of CL occurs within the temperature range of 100–190 °C. The temperature at 5 % mass loss ($T_{-5\%}$) of CL is 117 °C, and the temperature at the maximal decomposition rate (T_{dTGmax}) is 178 °C. On the other hand, the degradation of the reference PA6 commences at approximately 240 °C, leading to the breakage of the polymer chain. The $T_{-5\%}$ is 241 °C, and the T_{dTGmax} for PA6 is around 340 °C. The decomposition of expandable graphite starts above 200 °C, with the T_{dTGmax} occurring at 227 °C. The TGA tests also indicate the mode of action of the flame retardants, especially for condensed-phase flame retardants, as forming a charred protective layer reduces the mass loss rate. In the case of the condensed phase flame retardant EG, the mass loss of the sample clearly shows that at 600 °C, 75.7 % of the sample mass is retained due to the formation of a charred protective layer. HPCTP is a flame retardant acting mainly in the gas phase, so the residual mass is 0.5 % at 600 °C. The decomposition of HPCTP takes place between 300 and 450 °C, and the T_{dTGmax} is 381 °C.

As stated in the literature [38], above 200 °C, the detectable CL results from the decomposition of PA6 rather than from any unreacted residue. Therefore, the investigation of residual monomer content in the flame-retarded samples was conducted within the temperature range of 100–190 °C. The TGA analysis of the flame retardants reveals that the decomposition range of the flame retardants does not coincide with the decomposition range of CL. In the conversion calculation, we reduced the total mass by the mass of FRs. As it can be seen in Table 4, the monomer conversion of the reference and HPCTP-containing samples is between 97 and 98 %. Table 4 shows the TGA results for reference and PA6 with HPCTP. The TGA and DTG curves of PA6 with HPCTP are shown in Fig. 7.

HPCTP decreases the $T_{-5\%}$ value compared to the reference, but the $T_{-5\%}$ value can be increased by increasing the amount of the FR. With 4P% HPCTP, the $T_{-5\%}$ value reached 258 °C. In contrast, the temperature at 50 % mass loss was higher than in the case of PA6 reference in all flame retarded samples. The increase may be explained by the fact that the $T_{-50\%}$ of HPCTP (371 °C) is 30 °C higher than that of the reference PA6 (341 °C). Thus, $T_{-50\%}$ is also shifted towards higher temperatures for PA6 samples containing HPCTP. The value of $T_{-50\%}$ can be shifted by up to 21 °C with 1P% HPCTP. T_{dTGmax} increased only by a few degrees Celsius compared to the reference, while the dTG_{max} significantly decreased with HPCTP by up to 41 %. HPCTP mainly acts in the gas phase, which can be seen from the residual mass, as only PA6/1P%HPCTP showed an increase in residual mass compared to the reference.

3.1.3. Flame retardancy

The effect of HPCTP on the flammability of PA6 was investigated by

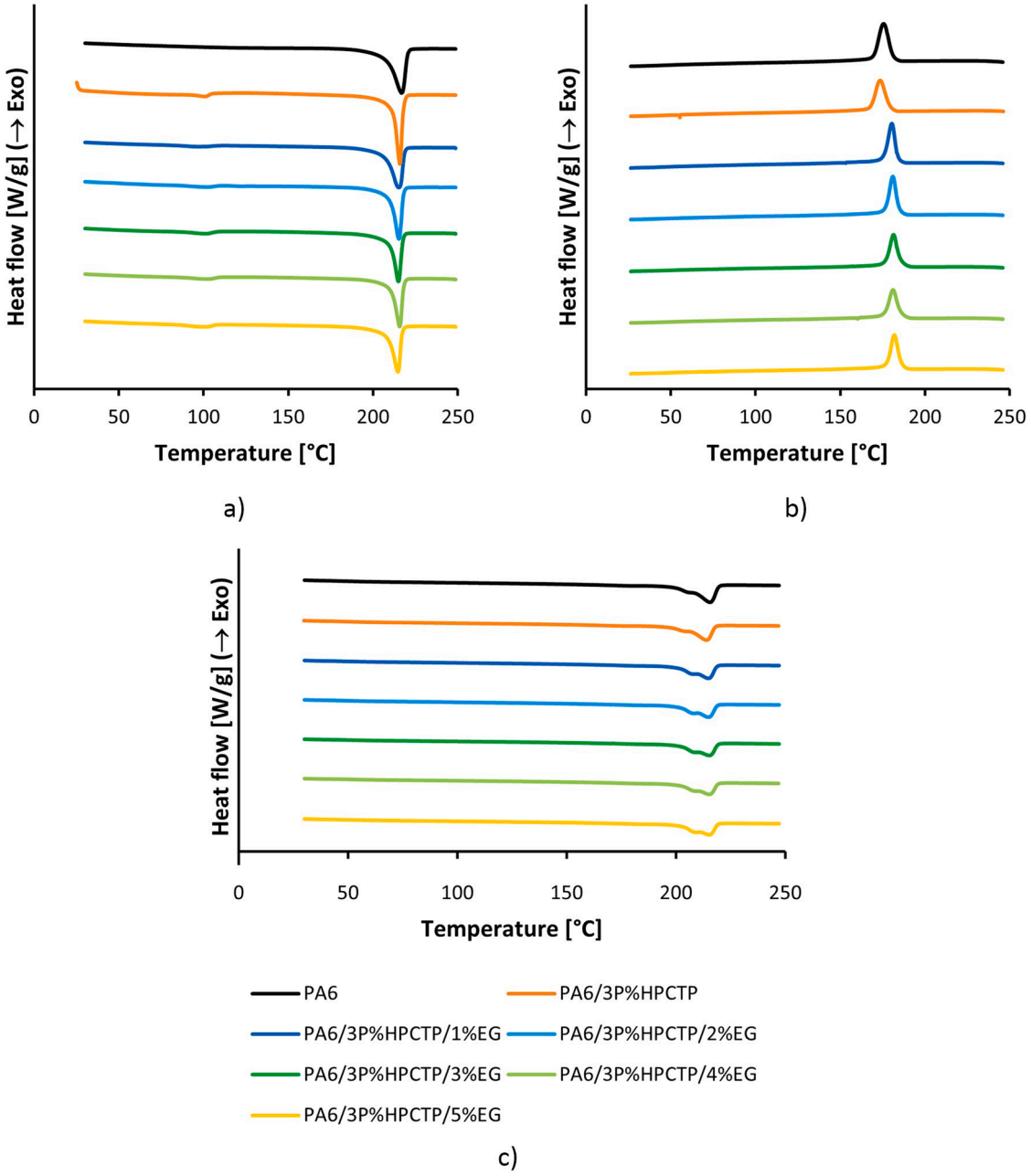

Fig. 9. DSC curves of PA6 with HPCTP and EG, where a) is the first heating, (b) is the cooling and (c) is the second heating.

UL-94 testing, LOI and MLC. The results of UL-94 and LOI are summarised in Table 5, while the results of MLC are shown in Table 6 and Fig. 8. For the MLC measurements, we determined the time to ignition (TTI), the peak heat release rate (pHRR) and the corresponding time (time to pHRR), the total heat release (THR), the residue, and the flame retardancy index (FRI) related to the reference PA6.

In the UL-94 test, all samples achieved an HB rating, but the burning rate decreased as the amount of HPCTP was increased. The burning rate was calculated using Eq. (2):

$$v = 60 \cdot \frac{L}{t} \tag{2}$$

where v is the burning rate [mm/min], L is the burning distance between the two marks (25 mm and 100 mm from the ignition point)[mm], and t is the burning time [s].

In addition to the decrease in the burning rate, it was observed that the damaged zone was also reduced. Also, the oxygen index value slightly increased by increasing the amount of the flame retardant.

The reference sample had peak heat release rate (pHRR) and total heat release rate (THR) values of 1019 kW/m^2 and 213 MJ/m^2, respectively. Only 4 %P HPCTP caused a significant decrease in pHRR of PA6, with the lowest pHRR value of 750 kW/m^2, equivalent to 26 % reduction. But this high amount of HPCTP led to an uneven sample surface and the sample could be easily broken by hand due to the plasticising effect of HPCTP. The THR values decreased by increasing the amount of flame retardants, with a reduction of up to 53 MJ/m^2 with 4P% HPCTP. In almost all cases, the ignition times for the samples containing HPCTP were practically identical to the reference sample. Only 4P% HPCTP showed a more significant increase in TTI (8 s). As with the TTI, no significant increase in pHRR time was observed, and except for 4 P% HPCTP, the TTI is reduced. The literature [23,24] suggests that HPCTP exerts its effects in condensed and gas phases.

Table 8
The results of TGA for flame retardant and reference PA6 samples ($T_{-5\%}$: the temperature at 5% mass loss; $T_{-50\%}$: the temperature at 50% mass loss; dTG_{max}: maximum decomposition rate; T_{dTGmax}: temperature corresponding to the maximum decomposition rate; Average standard deviation values: temperature measurements: ± 0.5 °C, mass measurements: ± 1%).

Sample	$T_{-5\%}$ [°C]	$T_{-50\%}$ [°C]	dTG_{max} [%/°C]	T_{dTGmax} [°C]	Char yield at 600 °C [%]	Monomer conversion [%]
PA6	241	341	2.1	338	2.0	97.5
PA6/3P% HPCTP	232	355	1.4	344	1.7	98.0
PA6/3P% HPCTP/ 1%EG	216	351	1.3	334	2.4	98.0
PA6/3P% HPCTP/ 2%EG	216	346	1.3	341	2.8	98.0
PA6/3P% HPCTP/ 3%EG	232	352	1.3	342	3.4	97.6
PA6/3P% HPCTP/ 4%EG	224	356	1.4	347	4.0	97.9
PA6/3P% HPCTP/ 5%EG	229	377	0.9	349	10.8	98.0

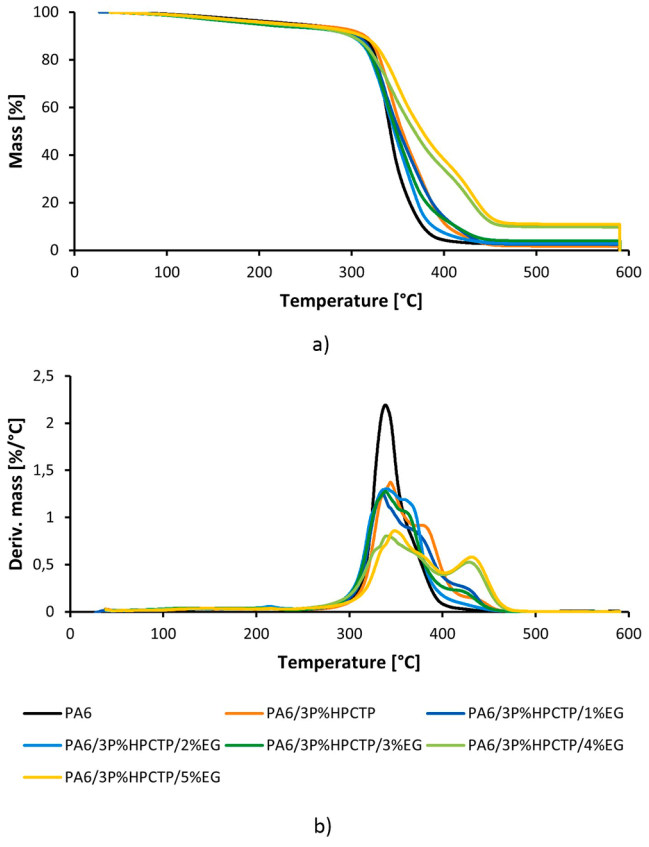

Fig. 10. TGA a) and DTG b) curves of PA6 with HPCTP and EG.

However, the residual mass indicates it is more effective in the gas phase. During the decomposition of PA6 containing HPCTP, the main chain of PA6 is breaks at elevated temperatures and free radicals are formed from HPCTP. Nitrogen-containing fragments are produced through intricate free radical reactions, leading to the formation of incombustible NH_3. Hydrocarbon pyrolysis and thermal oxydative decomposition also generate H_2O and CO_2, reducing combustible gases and oxygen concentration and producing a diluting effect [24].

Table 9
The results of UL-94 and LOI for reference and flame retardant coating materials (Average standard deviation of the LOI: ±1 vol%).

Sample	UL-94 ranking (burning rate)	LOI [%]
PA6	HB (24 mm/min)	21
PA6/3P%HPCTP	HB (6.9 mm/min)	24
PA6/3P%HPCTP/1%EG	HB (10 mm/min)	24
PA6/3P%HPCTP/2%EG	HB	26
PA6/3P%HPCTP/3%EG	HB	25
PA6/3P%HPCTP/4%EG	HB	25
PA6/3P%HPCTP/5%EG	V-0	28

The Flame Retardancy Index (FRI) of the samples was calculated to compare the flammability properties of each sample. The FRI was calculated using Formula 3:

$$FRI = \frac{\left(\frac{THR \cdot pHRR}{TTI}\right)_{reference}}{\left(\frac{THR \cdot pHRR}{TTI}\right)_{modified}} \quad (3)$$

Where THR [MJ/m^2] is the total heat release, pHRR [kW/m^2] is the peak heat release rate, and TTI [s] is the time to ignition.

The FRI is a dimensionless parameter widely used in the literature [39] to compare flame retarded and reference polymers. The FRI values were solely used for comparative purposes, with the flame retarded samples being compared to the reference. We used FRI solely to compare the samples containing HPCTP to the reference PA6. The FRI of the flame retarded samples increased slightly with the amount of HPCTP, but all together, the effect was modest.

From the MLC test results the maximum average rate of heat emission (MARHE) was determined. Compared to the reference value (638 kW/m^2s), HPCTP can reduce MARHE by up to 27 %. It was observed that the MARHE value showed a decreasing trend with the increase in the amount of flame retardant. A similar trend is observed for the effective heat of combustion. The EHC value decreases by 24 % with 4P% HPCTP (13 MJ/kg) compared to the reference (17 MJ/kg). The decrease in EHC is proportional to the increase in the amount of flame retardant.

3.2. PA6 coatings containing HPCTP and EG

The flammability tests revealed that HPCTP was effective as a standalone flame retardant additive, but did not show exceptional results. The sample containing 4P% HPCTP performed the best, but this amount of flame retardant was already visibly degrading the properties of PA6. For this reason, and to leverage the synergistic effects achievable through different modes of action, we combined 3P% HPCTP with expandable graphite.

3.2.1. Glass transition temperature and crystallinity

The effect of HPCTP and EG on the glass transition temperature, melting temperature and crystallinity was investigated by DSC. The results obtained are summarised in Table 7. The heating and cooling curves are shown in Fig. 9.

Based on the DSC results, it can be concluded that the combination of HPCTP and EG did not affect T_g and T_m. T_g was between 47 and 49 °C, while T_m was between 214 and 216 °C. By increasing the amount of EG, the ΔH_m gradually decreased. In general, ΔH_c increased as well, but no clear tendency could be observed; the crystalline fraction fluctuated between 43 and 53 %. Literature [40] suggests that EG may be a crystallisation site in PA6, increasing the crystalline fraction.

3.2.2. Thermal stability and monomer conversion

The thermal stability and monomer conversion of the mixed

Table 10
The results of MLC for reference and flame retardant coating materials (TTI: time to ignition, pHRR: peak heat release rate, THR: total heat release, FRI: flame retardancy index; Average standard deviation of the measured mass loss calorimeter values: TTI: ±3; pHRR: ±30; time to pHRR: ±5; residue: ±2).

Sample	TTI [s]	pHRR [kW/m^2]	time to pHRR [s]	THR [MJ/m^2]	Residue [%]	FRI [-]	MARHE [kW/m^{2}s]	EHC [MJ/kg]
PA6	19	1019	218	213	1.5	-	638	17
PA6/3P%HPCTP	23	987	202	182	0	1.4	557	14
PA6/3P%HPCTP/1%EG	27	489	302	174	3.3	3.6	360	31
PA6/3P%HPCTP/2%EG	22	399	360	168	5.3	3.7	286	30
PA6/3P%HPCTP/3%EG	42	400	375	166	7.8	7.2	265	30
PA6/3P%HPCTP/4%EG	26	327	353	151	9.8	6.0	203	27
PA6/3P%HPCTP/5%EG	26	336	345	151	7.6	5.9	264	27
PA6/4%EG	19	771	395	206	2	1.5	347	37

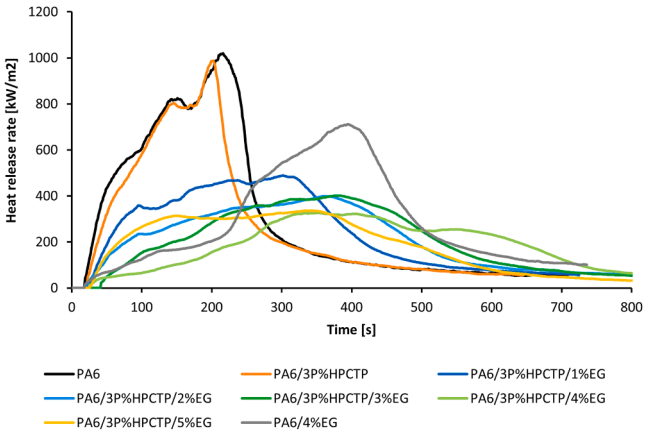

Fig. 11. The heat release rate of reference and flame retarded polyamide 6 with 3P% hexaphenoxycyclotriphosphazene (HPCTP) and different expandable graphite (EG) content.

composition samples were investigated by TGA. The results obtained are summarised in Table 8. The TGA and DTG curves of PA6 containing HPCTP and EG are shown in Fig. 10.

Compared to the reference value (241 °C), the $T_{-5\%}$ values were reduced by the flame retardants. With the combination of HPCTP and EG, the decomposition starts relatively early (216–232 °C), possibly due to the formation of a protective layer [35]. The improvement in thermal stability is suggested by the fact that $T_{-50\%}$ was shifted by up to 36 °C compared to the value of the reference sample (341 °C). 3 P% HPCTP and 1 % EG resulted in a slight decrease in T_{dTGmax}, but increasing the amount of EG led to a T_{dTGmax} of up to 349 °C, which is 11 °C higher than the relevant value of the reference. In addition, the d_{TGmax} was also reduced by the combined application of the FRs. The observed increase in the residual fraction indicates an improvement in thermal stability, which can be attributed to the increasing expandable graphite content. Using 5 % EG, a residual mass of 10.8 % was achieved. Monomer conversion was not affected by HPCTP and EG, leading to a conversion rate of 97–98 %.

3.2.3. Flame retardancy

The flammability of samples containing HPCTP and EG was tested by UL-94, LOI and MLC. The results of the UL-94 and LOI tests are summarised in Table 9. The MLC test results are given in Table 10, and the heat release curves are shown in Fig. 11.

Compared to the LOI of the sample containing only 3P% HPCTP (24 %), increasing the amount of expandable graphite further increased the LOI from 2 % EG content. The best result (28 %) was obtained with the PA6/3P%HPCTP/5 % EG sample, which also received the best V-0 grade according to UL-94. Only the PA6/3P%HPCTP/1 %EG sample burned until the first signal, and the others extinguished before, so we could only measure the burning rate for these samples. However, in the vertical test, all samples burned until clamping except the PA6/3P% HPCTP/5 % EG sample. Significant "worm-like" char formation was observed in both tests.

As shown in Fig. 11, the heat release of the reference PA6 sample and the sample containing 3 P% HPCTP after ignition increased significantly and a sharp peak at the maximum heat release was observed. In contrast, the heat release curves became flattened by the influence of EG, and the sharp peak at the maximum heat release was no longer observed. The time to ignition for all flame retarded samples was longer than in the case of the PA6 reference. The ignition was delayed by up to 23 s in PA6/3P%HPCTP/3 %EG sample compared to the TTI of the reference (19 s). The pHRR of the reference was 1019 kW/m^2, compared to which the flame retardants significantly reduced the maximum heat release in mixed compositions. The best-performing sample contained 3 P% HPTCT and 4 % EG ES100, with a maximum heat release of 327 kW/m^2. We further observed that the pHRR time of the specimens containing expandable graphite improved by more than one minute compared to the reference. The lowest THR values were obtained using HPCTP and 4 and 5 % expandable graphite. The total heat release of these samples was almost 30 % lower than that of the reference. The addition of EG led to a decrease in both the pHRR and the THR compared to the sample containing 3P% HPCTP alone, indicating the potential for a synergistic effect. By using a combination of EG and P-containing flame retardant, the P-containing flame retardant strengthens the char structure and provides an excellent protective layer against external heat flux for the unburnt raw material [34]. FRI values also improved compared to the sample with HPCTP only, with the best value obtained for PA6/3P% HPCTP/3 %EG. The sample containing 3 P% HPCTP and 4 % EG provided the highest amount of residue in the study, which was 9.8 % of the original total mass. Literature [41] suggests that by combining P-containing flame retardants with EG, phosphorus-containing products formed during their pyrolysis can increase the adhesion of EG bundles and the worming of EG-containing residues. A sticky coating is formed on the expandable graphite, limiting the volume increase and the mechanical stability of the refractory residue. High expandable graphite content is required to achieve the most efficient protective coating to provide an insulating volume increase.

In the case of MARHE, it can be observed that mixed compositions have also reduced the value compared to the reference. For PA6/3P% HPCTP/4 %EG samples, this reduction can be as high as 68 % compared to the reference PA6 (203 vs. 638 kW/m^{2}s). The significance of the combination of the two flame retardants is further demonstrated by the fact that MARHE was reduced by 36 % compared to the PA6/3P% HPCTP sample by the addition of only 1 mass% EG. In the case of EHC, an increase was observed with the addition of EG compared to both the reference PA6 and the PA6/3P%HPCTP sample. The addition of 1 mass % EG caused the EHC to increase by more than twofold compared to the PA6/3P%HPCTP sample.

For a proper comparison, the MLC results of the mixed composition coatings were compared with the sample containing only EG. Specifically, the sample containing 4 % EG was chosen for comparison because the PA6/3P%HPCTP/4 %EG sample had the lowest pHRR value of 327

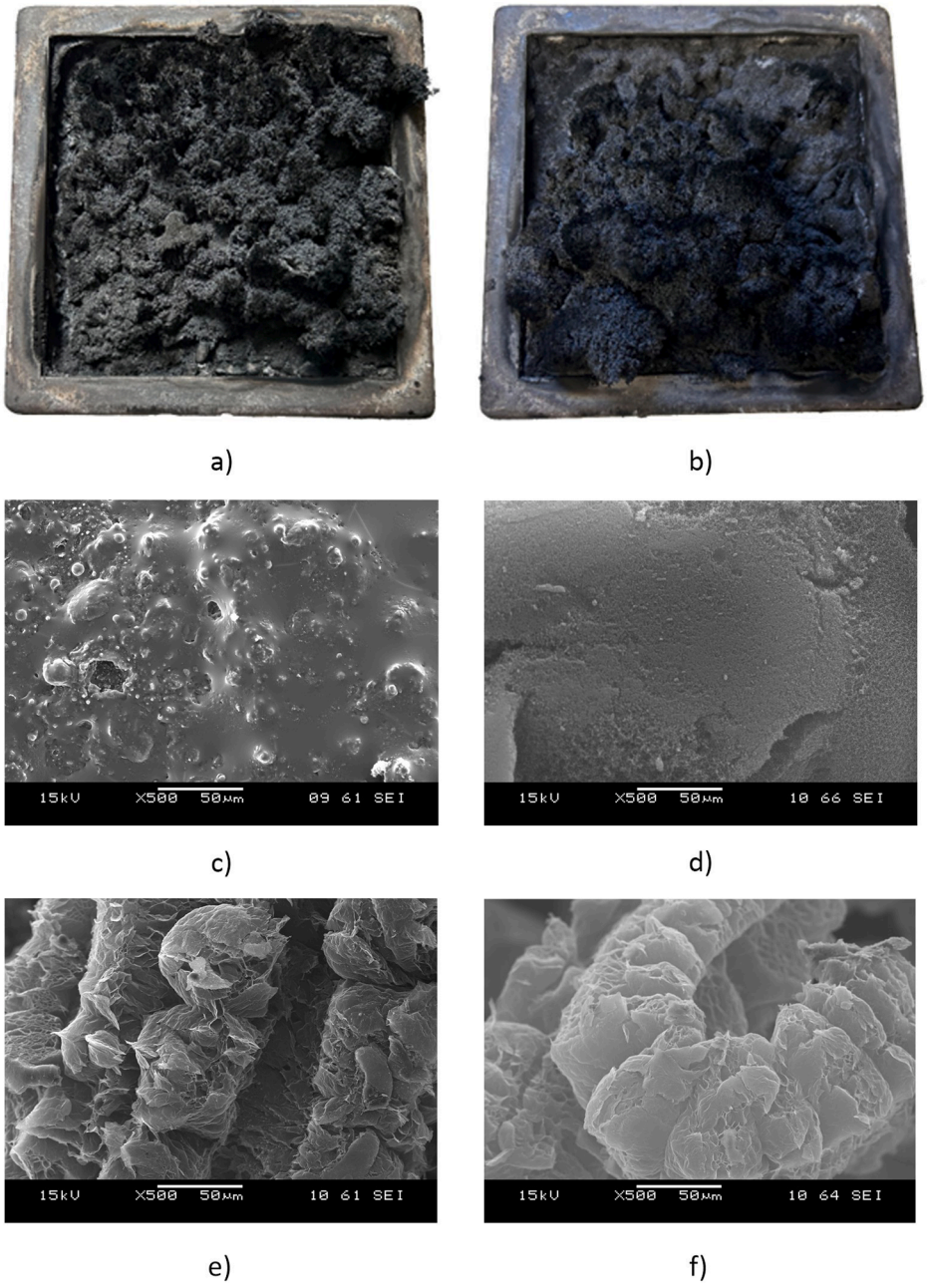

Fig. 12. Photographs taken after the MLC of PA6/3P%HPCTP/3 %EG a) and PA6/3P%HPCTP/4 %EG b), and SEM images of the outer part of the combustion residue for PA6/3P%HPCTP/3 %EG c) and PA6/3P%HPCTP/4 %EG d), and the inner part of the residue for PA6/3P%HPCTP/3 %EG e) and PA6/3P%HPCTP/4 %EG f).

Table 11
The results of MLC for reference and PA6 composite with flame retarded coating (TTI: time to ignition, pHRR: peak heat release rate, THR: total heat release; Average standard deviation of the measured mass loss calorimeter values: TTI: ±3; pHRR: ±30; time to pHRR: ±5; residue: ±2).

Sample	TTI [s]	pHRR [kW/m^2]	time to pHRR [s]	THR [MJ/m^2]	Residue [%]	FRI [-]
PA6/CF	17	347	164	95	32.5	5.9
PA6/CF/3P% HPCTP/3%EG	22	231	165	60	41.6	18.1
PA6/CF/3P% HPCTP/4%EG	36	261	92	57	41.5	27.7
PA6/CF/4%EG	25	295	78	99	44.9	9.8

kW/m^2.) Although the PA6/4 %EG sample ignited 7 s earlier than the PA6/3P%HPCTP/4 %EG sample, the pHRR time was shifted towards higher values (395 s). The pHRR of the mixed composition was 54 % lower than that of the PA6/4 %EG sample and 67 % lower than that of the PA6/3P%HPCTP sample. The post-combustion residue of the PA6/4 %EG sample is 2 %, the residue of the PA6/3P%HPCTP sample is 0 %, but the residue of the PA6/3P%HPCTP/4 %EG sample is 9.8 %. This suggests that HPCTP exhibits additional condensed phase effect when combined with EG. The MARHE value of the PA6/3P%HPCTP/4 %EG sample decreased by 42 % compared to PA6/4 %EG, while EHC decreased by 27 %.

Overall, the mixed composition samples can be used effectively to inhibit the combustion of caprolactam-based samples. Combining FRs with different modes of action can achieve a synergistic effect, and both maximum and total heat release can be significantly reduced.

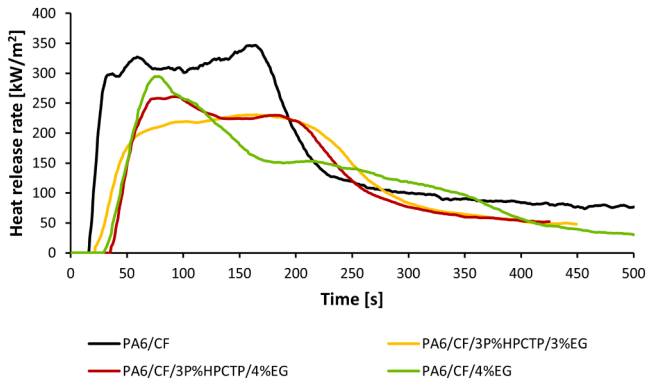

Fig. 13. The heat release rate of reference and flame retarded polyamide 6 composites with coatings containing hexaphenoxycyclotriphosphazene (HPCTP) and expandable graphite (EG).

After testing the different flame retardant formulations, two compositions that exhibited superior fire performance were chosen for further tests: PA6/3P%HPCTP/3 %EG and PA6/3P%HPCTP/4 %EG.

Photographs and SEM images of the two selected compositions after MLC are shown in Fig. 12.

In both samples, a more stable structure was observed on the outer side of the char, while the worm-like formations characteristic of expandable graphite were observed on the inside of the residue.

3.3. PA6/CF composites with flame retardant coatings

3.3.1. Flame retardancy

We applied the best-performing coatings on PA6 composites and tested the flammability of the coated samples by MLC. To investigate potential synergistic effects between HPCTP and EG, we also tested a composite coated with a formulation containing only EG. The results are shown in Table 11 and Fig. 13.

The reference uncoated carbon fibre-reinforced PA6 composite ignited in 17 s, while the TTI could be shifted by up to 19 s with the flame retardant coating. The sample with the coating containing 3 P% HPCTP and 4 % EG achieved the longest ignition time (36 s). The pHRR of the reference was 347 kW/m^2, compared to which both mixed coatings significantly reduced this value. The best-performing coating was the 3 P% HPCTP and 3 % EG, which reduced the pHRR of PA6 reference composite to 231 kW/m^2, equivalent to 33 % reduction. The coatings with mixed formulations reduced the total heat release of the composite samples by up to 37 %. The rerefence uncoated composite had a residual mass less than its original carbon fibre content (50 %), which may be explained by the fact that a hole was formed in the aluminium tray due to high heat emission. The coated samples have an increased residual mass compared to the reference, but even here, the residue does not reach 50 % because the fibre content is related to the uncoated composite and not to the total coated composite. The FRI of the samples was compared to the reference PA6 sample without fibre reinforcement. The mixed coatings significantly increased the FRI compared to the PA6/CF sample, the highest FRI was obtained for sample PA6/CF/3P%HPCTP/4 %EG (27.7). The flammability of the composite samples with mixed coatings was also compared to the PA6/CF/4 %EG sample without HPCTP. Given that we applied the coatings only in 0.5 mm thickness the differences are less pronounced than in the case of the coatings tested individually, still the benefits of the common application of HPCTP and EG are evident: The PA6/CF/3P%HPCTP/4 %EG sample ignited 11 s later than the PA6/CF/4 %EG sample and the pHRR occurred 14 s later. Compared with the PA6/CF/4 %EG sample, pHRR was reduced by 12 % and the THR by 43 % due to the effect of 3 %P HPCTP.

4. Conclusions

In our research, we developed flame retardant coatings for carbon fibre-reinforced ε-caprolactam-based PA6 composites. First, we investigated the effects of hexaphenoxycyclotriphosphazene (HPCTP), a flame retardant additive soluble in ε-caprolactam and not affecting its polymerisation, on the glass transition temperature, melting temperature, crystalline fraction, thermal stability, monomer conversion, and the flammability of PA6. The reference and flame retardant coating compositions were prepared by anionic ring-opening polymerisation of ε-caprolactam. The HPCTP did not significantly affect the glass transition temperature, the melting temperature, and the monomer conversion, but the crystalline fraction and thermal stability were increased. HPCTP as sole additive was effective, but did not exhibit exceptional flame retardancy, so it was combined with expandable graphite acting in the condensed phase. By combining HPCTP and EG, the maximum heat release was reduced by up to 68 % and the total heat release by 29 % compared to the PA6 reference. The results suggest that HPCTP exhibits additional condensed phase effect when combined with EG. Their joint application leads to a stable protective char layer upon ignition, which effectively insulates the material from the heat source and retards further combustion. The best-performing combined flame retardant formulations (PA6/3P%HPCTP/3 %EG, PA6/3P%HPCTP/4 % EGES100) were applied in 0.5 mm thickness on the surface of carbon fibre-reinforced PA6 composites by in-mould coating. With 0.5 mm coatings, the maximum heat release of PA6 composite was reduced by 33 % and the total heat release by 37 %. These findings highlight the potential of tailored flame retardant coatings in enhancing the safety and performance of thermoplastic composite materials, paving the way for their broader application in various industries.

CRediT authorship contribution statement

Zsófia Kovács: Writing – review & editing, Writing – original draft, Visualization, Validation, Resources, Investigation, Formal analysis. **Andrea Toldy:** Writing – review & editing, Visualization, Supervision, Resources, Project administration, Methodology, Funding acquisition, Conceptualization.

Declaration of competing interest

The authors declare that they have no known competing financial interests or personal relationships that could have appeared to influence the work reported in this paper.

Data availability

Data will be made available on request.

Acknowledgements

This research was funded by the National Research, Development and Innovation Office (2018–1.3.1-VKE-2018–00011 and NKFIH K142517). Project no. TKP-6–6/PALY-2021 has been implemented with the support provided by the Ministry of Culture and Innovation of Hungary from the National Research, Development and Innovation Fund, financed under the TKP2021-NVA funding scheme.

References

[1] G. Bánhegyi, Reconsidering plastics recycling and bio-plastics, Express Polym. Lett. 15 (2021) 685–686, https://doi.org/10.3144/expresspolymlett.2021.57.
[2] M. Valente, I. Rossitti, I. Biblioteca, M. Sambucci, Thermoplastic composite materials approach for more circular components: from monomer to *in situ* polymerization, a review, J. Compos. Sci. 6 (2022) 132, https://doi.org/10.3390/jcs6050132.

[3] O.V. Semperger, A. Suplicz, The degradation during recycling of polyamide 6 produced by anionic ring-opening polymerization of ε-caprolactam, Sci. Rep. 13 (2023) 17130, https://doi.org/10.1038/s41598-023-44314-0.
[4] S. Kuwashiro, N. Nakao, S. Matsuda, T. Kakibe, H. Kishi, Ionic cross-linked methacrylic copolymers for carbon fiber reinforced thermoplastic composites, Express Polym. Lett. 16 (2022) 116–129, https://doi.org/10.3144/expresspolymlett.2022.10.
[5] J. Lee, J.W. Lim, M. Kim, Effect of thermoplastic resin transfer molding process and flame surface treatment on mechanical properties of carbon fiber reinforced polyamide 6 composite, Polym. Compos. 41 (2020) 1190–1202, https://doi.org/10.1002/pc.25445.
[6] M.X. Li, H.L. Mo, S.K. Lee, Y. Ren, W. Zhang, S.W. Choi, Rapid impregnating resins for fiber-reinforced composites used in the automobile industry, Polymers 15 (2023) 4192, https://doi.org/10.3390/polym15204192 (Basel).
[7] A. Pegoretti, Towards sustainable structural composites: A review on the recycling of continuous-fiber-reinforced thermoplastics, Adv. Ind. Eng. Polym. Res. 4 (2021) 105–115, https://doi.org/10.1016/j.aiepr.2021.03.001.
[8] J. Chai, W. Feng, H. Yan, Y. Xia, Y. Yang, B. Wang, J. Li, Z. Fang, Z. Guo, Synergistic flame-retardancy of lamellar ceriumphenylphosphonate and aluminum diethylphosphinatetowards suppressing "candlewick effect" of polyamide6/carbon fiber composites (PDF) Synergistic flame-retardancy of lamellar cerium phenylphosphonate and alumi, J. Appl. Polym. Sci. 140 (2023) e54546, https://doi.org/10.1002/app.54546.
[9] Z. Kovács, Á. Pomázi, A. Toldy, The flame retardancy of polyamide 6—prepared by *in situ* polymerisation of ε-caprolactam—For T-RTM applications, Polym. Degrad. Stab. 195 (2022) 109797, https://doi.org/10.1016/j.polymdegradstab.2021.109797.
[10] A. Toldy, Flame retardancy of carbon fibre reinforced composites, Express Polym. Lett. 12 (2018) 186, https://doi.org/10.3144/expresspolymlett.2018.17.
[11] O.V. Semperger, D. Török, A. Suplicz, Development and analysis of an in-mold coating procedure for thermoplastic resin transfer molding to produce PA6 composites with a multifunctional surface, Period. Polytech. Mech. Eng. 66 (2022) 350–360, https://doi.org/10.3311/PPme.21048.
[12] G. Yang, W.H. Wu, Y.H. Wang, Y.H. Jiao, L.Y. Lu, H.Q. Qu, X.Y. Qin, Synthesis of a novel phosphazene-based flame retardant with active amine groups and its application in reducing the fire hazard of epoxy resin, J. Hazard. Mater. 366 (2019) 78–87, https://doi.org/10.1016/j.jhazmat.2018.11.093.
[13] S. Zhang, Y. Li, J. Guo, L. Gu, H. Li, B. Fei, J. Sun, X. Gu, Preparation of hexakis (4-aldehyde phenoxy) cyclotriphosphazene grafted kaolinite and its synergistic fire resistance in poly (butylene succinate), Polym. Compos. (2019) 1–12, https://doi.org/10.1002/pc.25434.
[14] M. Pan, R. Huang, T. Wang, D. Huang, J. Mu, C. Zhang, Preparation and properties of epoxy resin composites containing hexaphenoxycyclotriphosphazene, High Perform. Polym. 26 (2013) 114–121, https://doi.org/10.1177/0954008313501008.
[15] S.M. Seraji, H. Gan, S.R. Swan, R.J. Varley, Phosphazene as an effective flame retardant for rapid curing epoxy resins, React. Funct. Polym. 164 (2021) 104910, https://doi.org/10.1016/j.reactfunctpolym.2021.104910.
[16] L. Shen, J. Li, H. Lin, S. Feng, Y. Zhang, The enhanced compatibility and flame retarding ability of UHMWPE-MH composites by adding phenoxycyclophosphazene (HPCTP), Polym. Bull. 74 (2017) 3639–3655, https://doi.org/10.1007/s00289-017-1918-1.
[17] P. Zhang, D. Ma, J. Cheng, X. Zhang, X. Chen, Effects of hexaphenoxycyclotriphosphazene and glass fiber on flame-retardant and mechanical properties of the rigid polyurethane foam, Polym. Compos. 41 (2020) 3521–3527.
[18] L. Qu, Y. Sui, C. Zhang, X. Dai, P. Li, G. Sun, B. Xu, D. Fang, Improved flame retardancy of epoxy resin composites modified with a low additive content of silica-microencapsulated phosphazene flame retardant, React. Funct. Polym. 148 (2020), https://doi.org/10.1016/j.reactfunctpolym.2020.104485.
[19] H. Zhang, J. Tian, L. Yan, S. Zhou, M. Liang, H. Zou, Improving the ablation properties of liquid silicone rubber composites by incorporating hexaphenoxycyclotriphosphonitrile, Nanomaterials 13 (2023) 563, https://doi.org/10.3390/nano13030563.
[20] C. Lyu, M. Junqing, Y. Hou, L. Wang, J. Wang, Y. Lyu, Z. Zhou, A study on flame retardancy and smoke suppression of diatomite/hexaphenoxycyclotriphosphazene in silicone rubber foam, J. Rubber Res. 26 (2023) 407–413, https://doi.org/10.1007/s42464-023-00224-4.
[21] Y. Di, X. Wu, W. Wang, Experimental investigation of mechanical, thermal, and flame-retardant property of polyamide 6/phenoxyphosphazene fibers, J. Appl. Polym. Sci. (2019) 48458, https://doi.org/10.1002/APP.48458.
[22] L. Gao, X. Wu, Y. Di, Z. Zhao, W. Wang, X. Yin, Preparation and characterization of flame-retarded polyamide 6 fibers with hexaphenoxycyclotriphosphazene, J. Ind. Text. 51 (2021) 577–593, https://doi.org/10.1177/1528083719885013.
[23] C.C. Höhne, R. Wendel, B. Käbisch, T. Anders, Hexaphenoxycyclotriphosphazene as FR for CFR anionic PA6 via T-RTM a study of mechanical and thermal properties, Fire Mater. 41 (2016) 291–306, https://doi.org/10.1002/fam.2375.
[24] C. Yan, P. Yan, H. Xu, D. Liu, G. Chen, G. Cai, Y. Zhu, Preparation of continuous glass fiber/polyamide6 composites containing hexaphenoxycyclotriphosphazene: Mechanical properties, thermal stability, and flameretardancy, Polym. Compos. 43 (2021) 1022–1037, https://doi.org/10.1002/pc.26431.
[25] W.W. Focke, H. Muiambo, W. Mhike, H.J. Kruger, O. Ofosu, Flexible PVC flame retarded with expandable graphite, Polym. Degrad. Stab. 100 (2014) 63–69, https://doi.org/10.1016/j.polymdegradstab.2013.12.024.
[26] M. Modesti, A. Lorenzetti, Halogen-free flame retardants for polymeric foams, Polym. Degrad. Stab. 78 (2002) 167–173, https://doi.org/10.1016/S0141-3910(02)00130-1.
[27] W.W. Focke, H. Badenhorst, W. Mhike, H.J. Kruger, D. Lombaard, Characterization of commercial expandable graphite fire retardants, Thermochim. Acta 584 (2014) 8–16, https://doi.org/10.1016/j.tca.2014.03.021.
[28] F.M. Uhl, Q. Yao, H. Nakajima, E. Manias, C.A. Wilkie, Expandable graphite/polyamide-6 nanocomposites, Polym. Degrad. Stab. 89 (2005) 70–84, https://doi.org/10.1016/j.polymdegradstab.2005.01.004.
[29] M. Has, A. Erdem, L.A. Savas, U. Tayfun, M. Dogan, The influence of expandable graphite on the thermal, flame retardant and mechanical characteristics of short carbon fiber reinforced polyamide composites, J. Thermoplast. Compos. Mater. 36 (2023) 2777–2788, https://doi.org/10.1177/08927057221096656.
[30] F. Tomiak, A. Schoeffel, K. Rathberger, D. Drummer, A synergistic flame retardant system based on expandable graphite, aluminum (diethyl-)polyphospinate and melamine polyphosphate for polyamide 6, Polymers 13 (2021) 2712, https://doi.org/10.3390/polym13162712 (Basel).
[31] F. Tomiak, K. Rathberger, A. Schöffel, D. Drummer, Expandable graphite for flame retardant PA6 applications, Polymers 13 (2021) 2733, https://doi.org/10.3390/polym13162733 (Basel).
[32] Y.Y. Chan, B. Schartel, It takes two to tango: synergistic expandable graphite–phosphorus flame retardant combinations in polyurethane foams, Polymers 14 (2022) 2562, https://doi.org/10.3390/polym14132562 (Basel).
[33] S. Yang, J. Wang, S. Huo, M. Wang, J. Wang, B. Zhang, Synergistic flame-retardant effect of expandable graphite and phosphorus-containing compounds for epoxy resin: Strong bonding of different carbon residues, Polym. Degrad. Stab. 128 (2016), https://doi.org/10.1016/j.polymdegradstab.2016.03.017.
[34] L. Qian, F. Feng, S. Tang, Bi-phase flame-retardant effect of hexa-phenoxy-cyclotriphosphazene on rigid polyurethane foams containing expandable graphite, Polymer 55 (2014) 95–101, https://doi.org/10.1016/j.polymer.2013.12.015 (Guildf).
[35] Q. Pang, J. Deng, F. Kang, S. Shao, Effect of expandable graphite/hexaphenoxycyclotriphosphazene beads on the flame retardancy of silicone rubber foam, Mater. Res. Express 7 (2020) 055308, https://doi.org/10.1088/2053-1591/ab9250.
[36] Z. Kovács, A. Toldy, Synergistic flame retardant coatings for carbon fibre-reinforced polyamide 6 composites based on expandable graphite, red phosphorus, and magnesium oxide, Polym. Degrad. Stab. 222 (2024) 110696, https://doi.org/10.1016/j.polymdegradstab.2024.110696.
[37] J.E. Mark, Polymer Data Handbook, Oxford University Press, Oxford, 1999.
[38] S. Kurt, J. Maier, R. Horny, S. Horn, D. Koch, J. Moosburger-Will, Determination of the residual monomer concentration of ε-caprolactam in polyamide-6 using thermogravimetric analysis coupled with Fourier transform infrared spectroscopy gas analysis, J. Appl. Polym. Sci. 138 (2021) 50730, https://doi.org/10.1002/app.50730.
[39] H. Vahabi, B.K. Kandola, M.R. Saeb, Flame retardancy index for thermoplastic composites, Polymers 11 (2019) 407, https://doi.org/10.3390/polym11030407 (Basel).
[40] S. Zhou, L. Yu, X. Song, J. Chang, H. Zou, M. Liang, Preparation of highly thermally conducting polyamide 6/graphite composites via low-temperature *in situ* expansion, J. Appl. Polym. Sci. 131 (2014) 1–10, https://doi.org/10.1002/app.39596.
[41] A. Wilke, K. Langfeld, B. Ulmer, V. Andrievici, A. Hörold, P. Limbach, M. Bastian, B. Schartel, Halogen-free multi-component flame retardant thermoplastic styrene-ethylene-butylene-styrene elastomers based on ammonium polyphosphate – expandable graphite synergy, Ind. Eng. Chem. Res. 56 (2017) 8251–8263, https://doi.org/10.1021/acs.iecr.7b01177.